

Pixel-SAIL: Single Transformer For Pixel-Grounded Understanding

Tao Zhang^{1,2} Xiangtai Li¹ Zilong Huang¹ Yanwei Li¹ Weixian Lei¹
 Xueqing Deng¹ Shihao Chen² Shunping Ji² Jiashi Feng¹
¹ Bytedance Seed ² WHU

Project Page: <https://zhang-tao-whu.github.io/project/pixelsail>

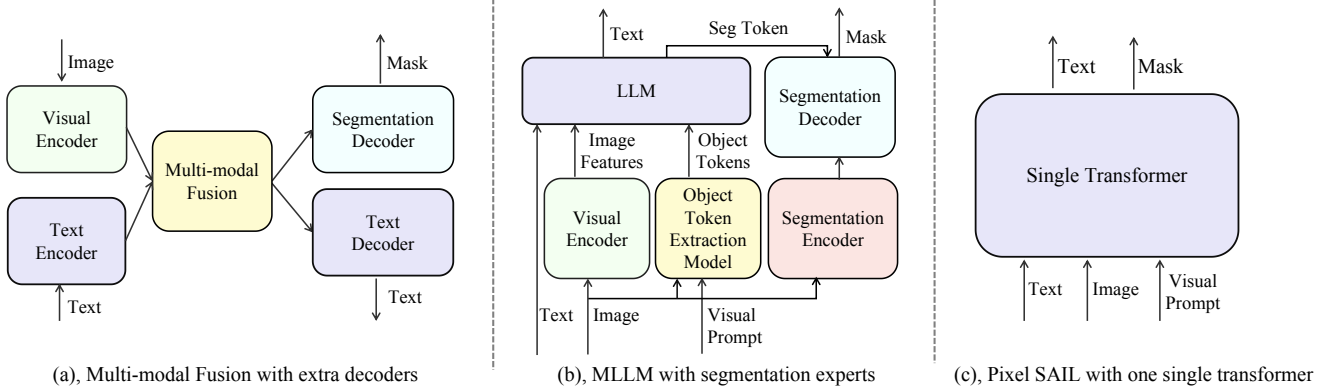


Figure 1. **Comparison of current MLLMs for pixel-wise understanding with our method.** (a) and (b). Current MLLMs for pixel-wise understanding feature highly complex system architectures, including an LLM, a CLIP-like vision backbone, an object token extraction model, a segmentation vision backbone, and a SAM-like decoder. (c). Our method employs only a single transformer.

Abstract

Multimodal Large Language Models (MLLMs) achieve remarkable performance for fine-grained pixel-level understanding tasks. However, all the works rely heavily on extra components, such as vision encoder (CLIP), segmentation experts, leading to high system complexity and limiting model scaling. In this work, our goal is to explore a highly simplified MLLM without introducing extra components. Our work is motivated by the recent works on Single trAnsformer as a unified vIsion-Language Model (SAIL) design, where these works jointly learn vision tokens and text tokens in transformers. We present Pixel-SAIL, a single transformer for pixel-wise MLLM tasks. In particular, we present three technical improvements on the plain baseline. First, we design a learnable upsampling module to refine visual token features. Secondly, we propose a novel visual prompt injection strategy to enable the single transformer to understand visual prompt inputs and benefit from the early fusion of visual prompt embeddings and vision tokens. Thirdly, we introduce a vision expert distillation strategy to efficiently enhance the single transformer’s fine-grained feature extraction capability. In addition, we have collected a comprehensive pixel understanding benchmark (PerBench), using a manual check. It includes three tasks:

detailed object description, visual prompt-based question answering, and visual-text referring segmentation. Extensive experiments on four referring segmentation benchmarks, one visual prompt benchmark, and our PerBench show that our Pixel-SAIL achieves comparable or even better results with a much simpler pipeline. Code and model will be released at <https://github.com/magic-research/Sa2VA>.

1. Introduction

Multi-modal Large Language Models (MLLMs) have garnered significant research efforts, driven by advancements of Large Language Models (LLMs) [22, 56, 65]. While most studies focus on open-ended visual question answering tasks, there is a growing interest [51, 80] in fine-grained, pixel-level understanding. This enables broader applications, such as facilitating precise region-level editing and generation and achieving precise understanding of designated mask regions.

Recent pixel-wise MLLMs [27, 51, 54, 63, 72, 80, 81] mainly adopt visual and language fusion frameworks, following design patterns [17, 42, 68] established before the LLM era. For example, LAVIT [68] adopts encoder-fusion approach, injecting language embedding (generated by BERT [13]) into vision transformers. With the advent of

LLMs [22, 65, 66], recent works [27, 54, 72, 80] integrate state-of-the-art segmentation models [26, 33, 53], for pixel-level understanding, by either appending them to LLM outputs or embedding LLM within segmentation pipelines. While effective, the overall architectures are complex, requiring specialized components such as vision-language fusion modules and additional decoders. Moreover, their final performance often heavily depends on either MLLMs or the segmentation models, which may lead to suboptimal results due to limitations within individual submodules.

In this work, we explore a novel, simple yet effective pixel-wise MLLM design, drawing inspiration from recent advancements in SAIL architecture, which is also called Encoder-free MLLMs. These methods drop the extra vision encoder and jointly co-train vision and language tokens on large scale datasets, with a simpler design. Moreover, they show competitive performance on image-level VQA tasks, compared with LLaVA. Motivated by this success, we extend the framework to pixel-level understanding tasks, aiming to reduce the complexity of existing approaches. To the best of our knowledge, this is the first study to explore the simplest architecture for pixel-wise MLLM tasks, including referring segmentation and visual prompt understanding.

We first directly extend SAIL architecture by adding segmentation token and visual prompt tokens to generate segmentation masks and output region caption, following previous works [27, 51, 74]. However, this leads to inferior results on both segmentation and visual prompt understanding. Several reasons are: (1), The misalignments on high resolution features since there are no segmentation decoders since SAIL directly reshape the vision tokens into features. (2), Previous works directly adopt mask pooling on high level visual tokens where SAIL baseline only maps RGB inputs with one projection layer, where most tokens are low level features. (3), The mask quality is low since no segmentation experts are involved.

To solve these problems, we present three simple technical improvements, which lead to our Pixel-SAIL framework. First, we design a simple learnable up-sampling module to refine the low resolution visual tokens in high resolution features. Our goal is to keep the design as simple as possible, where only one transposed 2D convolution is involved. Then, for visual prompt understanding, we design a novel visual prompt injection method, where we map the visual prompts into special text tokens without introducing extra visual prompt encoder in the middle stage of SAIL. Next, we propose to distill the previous segmentation experts into SAIL to improve mask quality. All the improvements are plug-in-play, and we verify the effectiveness on various SAIL architectures, including SOLO [8] and EVEv2 [16].

Then, to further indicate the effectiveness of our Pixel-SAIL and facilitate the development of pixel-LLM com-

munity, we further design a new challenging benchmark, PerBench. Compared with previous pixel-wise MLLM benchmarks, we have three innovative and challenging features. First, we include a detailed object caption where most existing benchmarks only contain short captions without fine-grained contents. Secondly, we re-evaluate visual-prompt understanding as multi-choice VQA tasks following MME [20] and MMBench [43] to achieve more accurate region caption evaluation. Thirdly, we introduce a task by segmenting objects jointly referenced by visual prompts and text. Our benchmark reveals the limitation of current state-of-the-art pixel-wise MLLM on fine-grained understanding and mixed referring tasks.

Pixel-SAIL is jointly co-trained with mixed data engine on referring segmentation datasets, VQA datasets, and visual prompt datasets. Experimental results show that our method can achieve better results on five pixel-wise benchmarks. In particular, on RefCOCOg and RefCOCO+ datasets, our method with 3B size can outperform previous pixel MLLMs, including GLaMM (7B) and OMG-LLaVA (7B), by 1.5-3.0%, with a simpler pipeline. On our PerBench, our method achieves 24.2 METEOR, 74% accuracy, 33.4 cIoU and 42.2 overall score, surpassing the SOTA MLLMs GLaMM (7B) and Sa2VA (4B) with overall scores of 26.9 and 3.2, respectively.

2. Related Work

Large Vision Language Models. Starting from CLIP [50] and ALIGN [24], modern vision language models have adopted contrastive learning on large-scale image-text datasets for learning vision-text aligned representations. The trained models are also proven to work well on open-vocabulary perception, such as segmentation [45, 71, 78, 79] and detection [21, 58, 61, 75]. The following works [31, 32, 64, 76] share the same network design, exploring modified loss functions and targeting data quality and filtering. Then, with the rise of large language models [5, 22, 56, 65], recent works [1, 10, 11, 40, 55, 77] mainly focus on multi-modal large language models for open-ended settings, such as visual question answering or OCR benchmarks. On representative work, LLaVA [40], uses the CLIP to encode images into visual tokens and sends the visual tokens to LLMs. After that, the following works [1, 30, 41] improve designs with scaled high quality datasets, images, and videos co-training. Meanwhile, several recent works [8, 14, 16, 46] also explore the visual encoder-free designs, which jointly learn the image and text representation in a single transformer architecture. For example, SOLO [8] collects mixed language and vision datasets and trains one transformer for VQA tasks, while EVE [14] designs a CLIP supervision to enhance visual token learning. Our work follows the visual encoder-free design, and we go a step further by exploring pixel-grounded understanding tasks, including ground-

ing tasks and visual prompt understanding. To our knowledge, we are the first to apply encoder-free architecture for pixel-grounded understanding tasks.

Referring Expression Segmentation. This task outputs specific masks driven by text description. Earlier works [19, 23, 36, 39, 67] explore various fusion architecture and modules to enhance text and vision feature alignments. Equipped with LLMs, several recent advanced works [27, 48, 49, 51, 63, 72, 73, 80, 82] propose more complex referring tasks, including reasoning referring or joint mask and caption generation. In particular, LISA [27] involves complex expression while GLaMM [51] annotates a new dataset and proposes region-level caption and segmentation tasks. However, all these works contain complex designs: extra vision encoders, segmentation encoders, mask decoders, and prompt encoders. Our method, Pixel-SAIL, only has one transformer to jointly learn the joint visual and language feature. With proposed data engine and improved methods, Pixel-SAIL achieves good results with much simpler architecture.

Visual Prompt Understanding. Understanding visual prompts plays an important role when building interaction between VLMs and human. Recent works [4, 38, 47, 51, 74] build new visual prompt datasets for region caption generation and prompt-aware VQA tasks. ViP-LLaVA [4] overlays the visual prompts directly onto the image canvas and fine-tunes the LLaVA on a specific visual prompt dataset, while Osprey [74] explores pixel-wise mask regions into language instructions. Our method can also be extended into visual prompt understanding with our proposed prompt token injection design.

3. Method

3.1. Encoder Free MLLM and Plain Baseline

Recently, several encoder-free MLLMs [8, 15, 16, 46] achieve comparable performance with those extra vision encoders. These models jointly learn vision and text features in a single transformer, with much simpler architecture. In particular, SOLO uses a simple project layer to map the image into visual tokens and then combines language tokens as the inputs of the transformer. However, no works have explored such new architecture for fine-grained vision language tasks (region caption, referring masks).

Plain Baseline. To fill this gap, we first construct a plain single transformer baseline, motivated by the previous ViT-based MLLMs [27, 72]. We start it with a pre-trained encoder-free MLLM. For segmentation tasks, we modify previous mask generation methods into the single transformer. First, we reshape the hidden states of the last transformer layer of vision tokens $\mathcal{V} \in \mathbb{R}^{N \times C}$ into image features $\mathcal{F} \in \mathbb{R}^{\frac{H}{S} \times \frac{W}{S} \times C}$. N represents the number of vision tokens, C denotes the channel size, H and W indicate

the height and width of the image, S stands for the down-sampling stride. Then, the image features are then cross-multiplied with the hidden states of the predicted segmentation token $\mathcal{Q} \in \mathbb{R}^{K \times C}$ to generate the segmentation masks $\mathcal{M} \in \mathbb{R}^{K \times \frac{H}{S} \times \frac{W}{S}}$. K signifies the number of predicted segmentation tokens, following previous works [27, 51]. For visual prompt understanding, we employ a pooling-based method [74] to derive object representations $\mathcal{O} \in \mathbb{R}^{M \times C}$ from image patch embeddings $\mathcal{P} \in \mathbb{R}^{\frac{H}{P} \times \frac{W}{P} \times C}$. These object embeddings are fed into the single transformer to represent the corresponding objects. M represents the number of visual prompts, and P denotes the patch size. For segmentation tasks, we adopt extra mask loss. Otherwise, we adopt the same text loss for VQA tasks and visual prompt understanding tasks.

Limitation. The plain baseline demonstrates a certain level of pixel-text alignment capability since both segmentation token and visual prompt token are jointly learned with vision and language tokens. However, the plain baseline exhibits several significant shortcomings: 1) The segmentation mask quality is poor due to the large feature down-sampling stride (16 or 32), even when using simple pixel shuffle or bilinear interpolation for up-sampling. 2) The single transformer struggles to comprehend the referential target of object representation, as the object representation is summarized from image patch embeddings with poor semantic information.

3.2. Pixel-SAIL Method

Given the substantial shortcomings, the performance of plain baseline in fine-grained pixel understanding tasks falls significantly, compared to vision-expert competitors (Sec.4). To solve these challenges, we have implemented three key enhancements to the baseline architecture. First, we integrate a learnable up-sampling module to fully exploit the segmentation capabilities of the single transformer architecture. Second, we develop an innovative visual prompt injection mechanism that facilitates effective interpretation of visual prompt inputs. Our method enables early-stage fusion between vision tokens and visual prompt embeddings. Finally, we introduce a dense feature distillation strategy that significantly improves the model’s capacity for extracting fine-grained visual features. These improvements collectively address the shortcomings of the plain baseline while maintaining its architectural simplicity.

Learnable Up-sampling Module. Inspired by [35], we also incorporate a simple learnable up-sampling model \mathcal{U} to generate the high-resolution features $F_h \in \mathbb{R}^{\frac{H}{4} \times \frac{W}{4} \times C}$ essential for pixel-level grounding. The up-sampling module comprises multiple up-sampling blocks, each consisting of a transposed 2D convolution followed by a depth-wise convolution. It effectively upscales the low-resolution features $F_l \in \mathbb{R}^{\frac{H}{S} \times \frac{W}{S} \times C}$, derived from resized vision tokens,

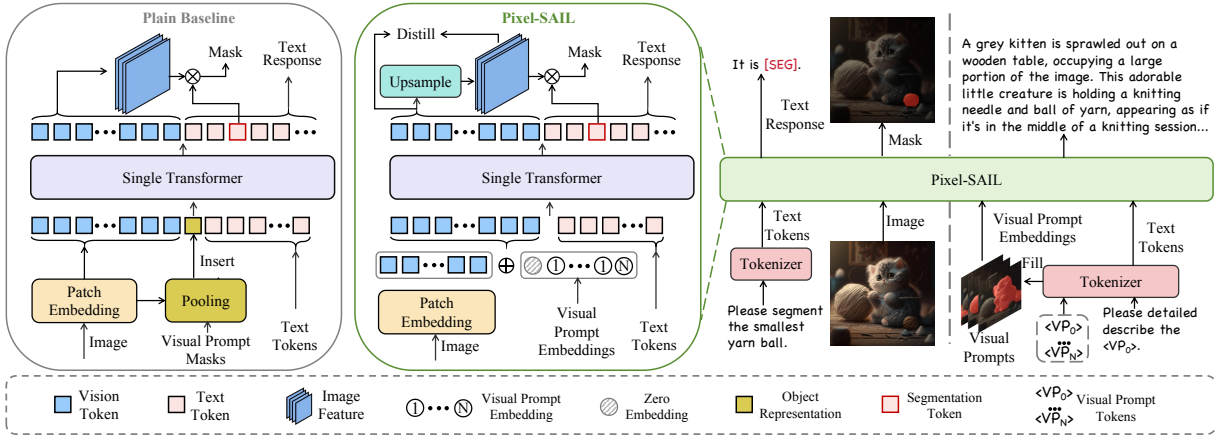


Figure 2. **The architecture of our proposed plain baseline and Pixel-SAIL.** Pixel-SAIL is as simple and elegant as the plain baseline but demonstrates significantly improved performance. The examples on the right demonstrate that Pixel-SAIL possesses the capability for general conversation and comprehensive pixel-grounded understanding.

to one-quarter of the original resolution.

Visual Prompt Injection. Previous works [51, 72, 74] summarize the referenced object features via pooling on vision tokens from ViT encoder. However, there are no such visual tokens for encoder-free MLLMs. Thus, the inherent semantic deficiency hinders the single transformer’s ability to precisely identify referenced objects based solely on feature summaries derived from patch embeddings, where most are low-level cues, such as edges.

To overcome this limitation, we propose an innovative visual prompt injection mechanism. Our approach integrates multiple visual prompt special tokens $\{VP_i | i \in [1, N]\}$ into the large language model’s vocabulary. These tokens’ text embeddings $\mathcal{VP}^t \in \mathbb{R}^{N \times C}$ are used to fill mask-based visual prompts $\mathcal{M}^{vp} \in \mathbb{R}^{N \times \frac{H}{P} \times \frac{W}{P}}$, thereby creating visual prompt tokens $\mathcal{VP} \in \mathbb{R}^{\frac{HW}{P^2} \times C}$. The vision tokens $\mathcal{V} \in \mathbb{R}^{\frac{HW}{P^2} \times C}$ are first added with these visual prompt tokens \mathcal{VP} before being processed by the single transformer. This enhancement enables the model to accurately identify referenced objects by leveraging the corresponding special tokens $\{VP_i | i \in [1, N]\}$ within the text instructions.

Dense Feature Distillation. Due to the lack of large-scale, high-quality segmentation data like SA-1B [26], the method produces poor-quality masks, particularly at object boundaries. However, directly training on large-scale segmentation datasets would be costly and damage the original instruction following capabilities. To address both, we employ pre-trained segmentation experts to distill the single transformer, ensuring optimization of object details without hurting VQA capabilities. We perform distillation by leveraging mask features generated by Mask2Former’s [12] pixel decoder on the upsampled mask features $F_h \in \mathbb{R}^{\frac{H}{4} \times \frac{W}{4} \times C}$, and utilizing features produced by SAM2’s [53] encoder

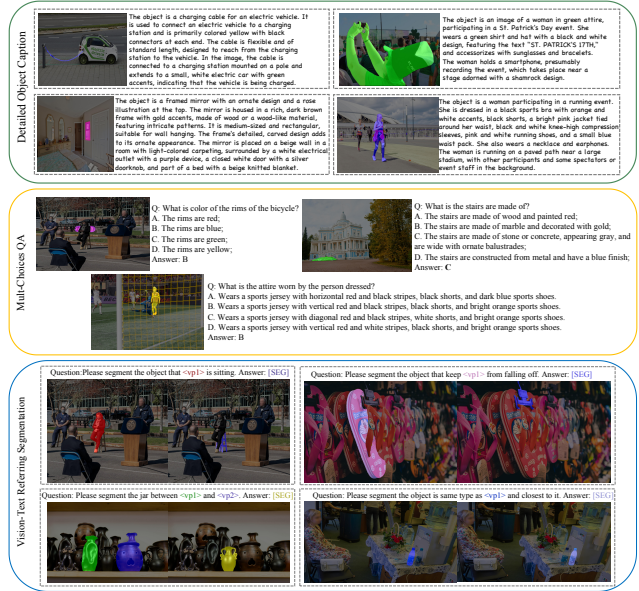


Figure 3. **Visual examples on our PerBench. Best view it in color and zoom in.**

on the low-resolution features $F_l \in \mathbb{R}^{\frac{H}{8} \times \frac{W}{8} \times C}$. This simple distillation strategy improves segmentation quality with only a negligible increase in training time.

3.3. Benchmark and Dataset Engine

Our Benchmark: PerBench. We further manually annotate a benchmark named **PerBench** (Pixel-grounded Understanding Benchmark). PerBench aims to address three aspects lacking in existing pixel grounding benchmarks.

The first aspect is detailed object caption. Previous works [6, 34] have emphasized more detailed image captions, demonstrating that comprehensive captions signifi-

cantly enhance model performance. However, current object caption datasets such as Osprey-724k [74] and evaluation benchmarks like Refcocog provide only cursory object captions. To address this limitation, we leverage SOTA models InternVL2.5-78B [11] and Qwen2.5VL-72B [2] to generate detailed object captions. These detailed object captions are then meticulously screened and refined through **manual review**, ultimately yielding 500 precise, nuanced object captions to serve as a robust evaluation benchmark. METEOR [3] serves as the evaluation metric for the detailed object caption task.

The second aspect is the assessment of visual-prompt understanding ability in multiple-choice format. Although captioning tasks can accurately reflect a model’s visual prompt understanding ability, precise and fair evaluation is difficult. Rule-based metrics such as CIDEr [57] and METEOR [3] are affected by response length, format, and ground-truth quality, while using models as evaluators inevitably introduces model bias. Therefore, a fair and quantitative visual-prompt understanding benchmark is necessary. Inspired by MMBench [43] and MME [20], we manually annotated 500 multiple-choice questions based on detailed object captions, covering the examination of models’ understanding of referenced objects’ appearance, attributes, uses, and relationships with surrounding objects. MLLMs need to perceive the attributes of referenced objects accurately and have instruction-following ability to select the appropriate choice correctly. Accuracy is selected as the evaluation metric for the visual prompt-based multiple-choice questions.

The third aspect is segmenting objects jointly referenced by visual prompts and text, abbreviated as V-T RES. It aims to test the model’s ability to understand objects indicated by user-input visual prompts and segment associated objects according to text instructions. This task comprehensively assesses the MLLM’s pixel-grounded understanding ability, requiring the model to possess precise visual prompt understanding capabilities, text reasoning abilities, and pixel grounding skills. We also manually annotate 500 V-T RES samples, which five expert annotators double-check. Similar with RefCOCO series datasets, we select cIoU and gIoU as the evaluation metric for V-T RES task. The overall score of PerBench is the average of the normalized scores (0-100) from the above three tasks.

Our benchmark can be used to evaluate pixel-wise MLLMs and point out more challenging directions for detailed object understanding, joint visual prompts, and text understanding to the current community.

Dataset Engine. To fully unleash the potential of the single transformer, we collect diverse pixel-grounded data, including segmentation datasets and visual-prompt understanding datasets, following previous works [16, 46].

For segmentation-related data, we first use Ref-

COCO+/g [25, 70] and COCO [37] semantic segmentation data used in LISA [27], the Grandf dataset (214k samples) used in GLaMM [51], and MUSE data (246k samples) used in PixelLM [54]. We also use recent Pixel2Cap [69] data (comprising 20k images) and organized it into the referring segmentation format. Finally, we further add COCO [37] panoptic segmentation data and structured it as: “*Question: Please segment the {class name} in instance mode. Answer: {class name}-1 [SEG], ..., {class name}-n [SEG].*”

For visual prompt understanding, we employ two public datasets: Osprey-724k [74] and Pixel2Cap [69]. Additionally, we reformat the COCO dataset into a question-answer structure specifically designed to query object categories. To enhance the model’s capability for fine-grained object description, we prompt the InternVL2.5-78B [11] model to generate approximately 300k detailed object captions derived from 10k SA-1B [26] images. Lastly, to maintain the instruction following ability, we also integrate the LLaVA-1.5 [40] 665k dataset into our training data.

Training. We combine all the aforementioned data for co-training. The loss function consists of the next token prediction loss \mathcal{L}_{ntp} , the segmentation loss \mathcal{L}_{seg} , and the distillation loss $\mathcal{L}_{distill}$:

$$\mathcal{L} = \mathcal{L}_{ntp} + \mathcal{L}_{seg} + \alpha \mathcal{L}_{distill}, \quad \mathcal{L}_{seg} = \lambda \mathcal{L}_{ce} + \beta \mathcal{L}_{seg}, \quad (1)$$

where α is set to 0.5, λ to 2.0 and β to 0.5.

4. Experiment

Implementation Details. We extensively evaluate our meta-architecture using two open-source encoder-free multimodal large language models: SOLO [8] and EVEv2 [16]. For SOLO, following [28], we modify the attention mechanism between vision tokens from causal attention to full attention and conduct supervised fine-tuning on the LLaVA-1.5 665k dataset. For SOLO, we modify the attention mechanism between vision tokens from causal attention to full attention and replace the LLM with Qwen2.5 [66] 0.5B and 3B, respectively. For EVEv2, we retain its original architecture and weights without any modifications. We build Pixel-SAIL 0.5B and 3B based on our modified SOLO baseline, and 7B on EVEv2. When training Pixel-SAIL based on SOLO, we maintain the original resolution of input images. For images with a long side exceeding 1024, we preserve the aspect ratio and resize the long side to 1024. When training Pixel-SAIL based on EVEv2, we resize the images to the closest to 800^2 pixels to reduce training costs, which differs from the original setting of 1600^2 . The training process is conducted on 32 A100 (80GB) GPUs using the AdamW [44] optimizer with a cosine decay learning rate scheduler. We set the initial learning rate to $4e-5$, the warm-up ratio to 0.03, and the batch size to 256. The training duration for the 0.5B and 3B models is 12 hours and 24 hours, respectively.

Table 1. **Performance on referring segmentation benchmarks.** The evaluation metric is cIoU. “ft” denotes fine-tuning on the specific dataset.

Method	LLM Size	RefCOCO+			RefCOCOg		RefCOCO			gRefCOCO		
		val	testA	testB	val(U)	test(U)	val	testA	testB	val	testA	testB
Referring Segmentation Specialist Without MLLM												
VLT [17]	-	56.3	61.0	50.1	55.0	57.7	67.5	70.5	65.2	52.5	62.2	50.5
CRIS [59]	-	62.3	68.1	53.7	59.9	60.4	70.5	73.2	66.1	55.3	63.8	51.0
LAVT [68]	-	62.1	68.4	55.1	61.2	62.1	72.7	75.8	68.8	57.6	65.3	55.0
PolyFormer-L [42]	-	69.3	74.6	61.9	69.2	70.2	76.0	78.3	73.3	-	-	-
ReLA [39]	-	66.0	71.0	57.7	65.0	66.0	73.8	76.5	70.2	56.4	59.0	58.4
MLLMs With Vision Expert												
LISA (ft) [27]	7B	65.1	70.8	58.1	67.9	70.6	74.9	79.1	72.3	-	-	-
PixelLM [54]	7B	66.3	71.7	58.3	69.3	70.5	73.0	76.5	68.2	-	-	-
GSVA (ft) [63]	7B	64.5	67.7	58.6	71.1	72.0	76.4	77.4	72.8	61.7	69.2	60.3
GroundHog [81]	7B	70.5	75.0	64.9	74.1	74.6	78.5	79.9	75.7	66.7	-	-
GlaMM (ft) [51]	7B	72.6	78.7	64.6	74.2	74.9	79.5	83.2	76.9	-	-	-
SAM4MLLM [9]	7B	73.5	77.8	65.8	74.5	75.6	79.6	82.8	76.1	66.3	70.1	63.2
LaSagna [60]	7B	66.4	70.6	60.1	70.6	71.9	76.8	78.7	73.8	38.1	50.4	42.1
OMG-LLaVA (ft) [80]	7B	69.1	73.1	63.0	72.9	72.9	78.0	80.3	74.1	-	-	-
F-LLM [62]	7B	65.8	75.2	58.5	70.1	71.7	75.8	79.5	72.4	-	-	-
Sa2VA [72]	4B	74.3	-	-	76.7	-	80.4	-	-	-	-	-
MLLMs Without Vision Expert												
Pixel-SAIL	0.5B	70.8	75.8	65.4	75.4	76.7	77.9	80.5	75.9	63.9	71.5	63.6
Pixel-SAIL (ft)	0.5B	73.0	77.0	68.0	75.6	76.1	79.1	81.7	77.0	68.0	74.0	66.8
Pixel-SAIL	3B	75.7	79.7	72.0	78.7	80.4	80.8	82.6	79.0	67.7	74.6	67.1
Pixel-SAIL (ft)	3B	76.2	79.7	71.2	78.5	79.4	81.8	83.4	78.8	72.1	77.1	70.4

Table 2. **Region caption performance on RefCOCOg dataset.**

Method Size	Pixel-SAIL 0.5B	Pixel-SAIL 3B	Sa2VA 4B	OMG-LLaVA 7B	Osprey 7B	GLaMM 7B
METEOR	16.0	17.6	17.3	15.3	16.6	16.2

Table 3. **The performance on our PerBench.** Due to the lack of visual prompt understanding capability, LISA scores 0 on all tasks.

Model	Size	Detailed Caption METEOR	MCQ Acc	V-T RES		Overall Score
				cIoU	gIoU	
LISA [27]	7B	0	0	0	0	0
Osprey [74]	7B	13.4	0.12	0	0	8.5
GLaMM [51]	7B	12.6	0.14	24.3	14.6	15.3
Sa2VA [72]	4B	19.2	0.71	31.9	21.9	39.0
Pixel-SAIL	0.5B	21.4	0.69	29.7	19.8	38.4
Pixel-SAIL	3B	24.2	0.74	33.4	23.5	42.2

Table 4. **Performance on the VQA benchmarks.** * refers to the use of an 800² resolution, which differs from the 1600² resolution in the pre-trained model.

Model	LLM Size	MME	MMBench	SEED	MMStar
SOLO	0.5B	523.2/222.5	13.8	45.5	26.2
SOLO	3B	1155.7/257/5	53.4	65.4	40.3
EVEv2*	7B	1128.0/240.7	60.3	54.2	44.9
Pixel-SAIL	0.5B	564.1/150.7	31.8	52.2	26.3
Pixel-SAIL	3B	1187.3/242.9	56.3	66.1	40.1
Pixel-SAIL*	7B	1081.0/260.4	58.9	64.7	44.3

Evaluation Setup. For visual prompt understanding and general image QA tasks, we adhere to the same setting as the base MLLM. In the case of segmentation-related tasks, if the model fails to predict a [SEG] token, we compel it

to produce a [SEG] token to ensure the generation of the segmentation result.

4.1. Main Results

Results on Referring Segmentation Benchmarks. We compare Pixel-SAIL with other pixel-grounded MLLMs and segmentation specialists on the RefCOCO+ [70], RefCOCOg [70], RefCOCO [25], and gRefCOCO [39] datasets. The comparison results are shown in Tab. 1. Pixel-SAIL 0.5B achieved 70.8, 75.4, and 77.9 cIoU on the validation splits of RefCOCO+, RefCOCOg, and RefCOCO, outperforming all segmentation specialists with comparable model sizes while also maintaining image conversation capabilities. Compared to the classical SAM-based MLLM competitor LISA-7B [27], Pixel-SAIL 0.5B surpassed it by 4.2, 7.9, and 7.8 cIoU on RefCOCO, RefCOCO+, and RefCOCOg respectively, despite having a much smaller model size (0.5B vs. 7B). On the more complex gRefCOCO dataset that includes multi-object segmentation, Pixel-SAIL 0.5B outperformed the carefully designed GSVA-7B [63] by 6.3, 4.8, and 6.5 cIoU on validation, testA, and testB splits respectively.

When scaling the model to 3B, Pixel-SAIL achieved 75.7, 78.7, 80.8, and 67.7 cIoU on RefCOCO+, RefCOCOg, RefCOCO, and gRefCOCO datasets respectively, surpassing all larger-sized (7B) MLLMs assisted with vision experts. Pixel-SAIL-3B even outperformed the SOTA Sa2VA-4B [72] (which uses the powerful InternVL2-

ule, segmentation quality improves dramatically, with the model reaching 76.2, 69.6, and 73.8 cIoU on RefCOCO, RefCOCO+, and RefCOCOg. However, the model still cannot effectively interpret user-input visual prompts due to insufficient semantic information in the object representation. When we scale up the training data by introducing substantial amounts of segmentation data and visual-prompt understanding data, the model’s segmentation capabilities are further enhanced. Despite scaling the training data, the model continues to struggle with visual prompt inputs because of the limited semantic information in the object representation. After implementing our proposed visual prompt injection mechanism, the model demonstrates significant improvements in visual prompt understanding, achieving 16.1 METEOR on the region caption task. Interestingly, we observe that enhanced visual prompt understanding capabilities positively influence referring segmentation performance. Finally, incorporating the distillation strategy further refines the model’s detailed segmentation quality.

Ablation on Various MLLMs. To demonstrate the effectiveness of Pixel-SAIL, we validate across different architectures and sizes, with results shown in Tab. 6. To reduce training costs, we use only LLaVA-665k and RefCOCO+/g data for training and evaluate on the referring segmentation task. When using our modified 0.5B SOLO as the base MLLM, Pixel-SAIL achieves cIoU scores of 69.7, 62.5, and 65.3 on RefCOCO+/g. When scaling the model size to 3B, Pixel-SAIL’s performance improves by 3.5, 3.9, and 3.8 cIoU on RefCOCO+/g. When using EVEv2-7B as the base MLLM, despite the attention between vision tokens changing from full attention to causal attention and the architecture transitioning to an MOE architecture, Pixel-SAIL achieves cIoU scores of 77.4, 70.4, and 75.2 on RefCOCO+/g, demonstrating that performance consistently increases with model scaling.

Ablation on Data Scaling. Data plays a crucial role in the performance of Pixel-SAIL. As shown in Tab. 7, we conduct comprehensive ablation studies on the training data to evaluate its impact. When trained solely with basic data (including LLaVA-665k and RefCOCO+/g datasets), Pixel-SAIL achieves 69.7, 62.5, and 65.3 cIoU on RefCOCO, RefCOCO+, and RefCOCOg, respectively. Upon scaling the segmentation-related data, Pixel-SAIL demonstrates significant performance improvements of 6.5, 7.1, and 8.5 cIoU on these datasets. Furthermore, incorporating visual prompt data for mixed training not only enhances the model’s visual prompt understanding capabilities but also yields additional performance gains of 1.2, 0.8, and 1.4 cIoU on RefCOCO, RefCOCO+, and RefCOCOg, respectively.

Ablation on Distillation Strategy. Distillation is a highly effective method for infusing knowledge into Pixel-SAIL. We conduct ablation studies on the distillation strategy, and

the results are presented in Tab. 8. We use the average cIoU across all splits as the evaluation metric. When only Mask2Former [12] is employed to distill high-resolution mask features, Pixel-SAIL achieves performance gains of 0.2, 0.5, and 0.3 on RefCOCO+/g. When SAM2 [53] is used to distill low-resolution image features, Pixel-SAIL obtains performance improvements of 0.3, 0.4, and 0.4 on RefCOCO+/g. When both teacher models are utilized collaboratively, performance gains of 0.6, 0.3, and 0.5 are achieved. Additionally, the extra computational cost introduced by the distillation strategy is minimal, increasing the training time by only about 5% for Pixel-SAIL-0.5B.

4.3. Visualization Analysis

Visual Comparison. In Fig. 4, we showcase Pixel-SAIL’s visualization results on diverse tasks. Pixel-SAIL flexibly interprets both visual prompts and text instruction inputs, responding with text and segmentation masks.

Visual Affinity Map Analysis. We use PCA dimensionality reduction algorithm to visualize vision features, with results shown in Fig. 5. Our Pixel-SAIL’s image features (3rd column) are denser and more diverse compared to the base MLLM’s image features (2nd column). Pixel-SAIL’s mask features, after the upsampling module, are denser and have better segmentation edges. Interestingly, Pixel-SAIL’s image features (more focused on understanding, combining factors such as categories, colors, positions, etc.) exhibit different characteristics from mask features (more focused on perception, categories, and instances). As seen in the second row’s third and fourth columns, the cars on the left and right have relatively distant feature representations in the image features, while they are very close in the mask features.

5. Conclusion

We explore the simplest architecture for pixel-grounded understanding tasks. In particular, we present Pixel-SAIL, which extends current SAIL-like MLLM for fine-grained understanding with three technical improvements (learnable upsampling module, new visual prompt encoding, and segmentor feature distillation). For the first time, our work proves that even without extra visual experts (visual encoder, segmentation models), one single transformer can still achieve stronger performance on four public referring segmentation benchmarks. We further introduce a more challenging benchmark, Perbench, to promote the development of pixel-MLLM community.

Limitation and Future Work. Our work provides the simplest solution for pixel-grounded tasks. However, one limitation is that we only adopt 1.7M data for co-training. We will further explore Pixel-SAIL on more data (for example, billion-level masks along with visual prompts [26]) for co-training.

References

- [1] Jinze Bai, Shuai Bai, Shusheng Yang, Shijie Wang, Sinan Tan, Peng Wang, Junyang Lin, Chang Zhou, and Jingren Zhou. Qwen-vl: A versatile vision-language model for understanding, localization, text reading, and beyond. *arXiv preprint arXiv:2308.12966*, 2023.
- [2] Shuai Bai, Keqin Chen, Xuejing Liu, Jialin Wang, Wenbin Ge, Sibao Song, Kai Dang, Peng Wang, Shijie Wang, Jun Tang, et al. Qwen2. 5-vl technical report. *arXiv preprint arXiv:2502.13923*, 2025.
- [3] Satantjeev Banerjee and Alon Lavie. Meteor: An automatic metric for mt evaluation with improved correlation with human judgments. *ACL*, 2005.
- [4] Mu Cai, Haotian Liu, Siva Karthik Mustikovela, Gregory P. Meyer, Yuning Chai, Dennis Park, and Yong Jae Lee. Making large multimodal models understand arbitrary visual prompts. In *CVPR*, 2024.
- [5] Zheng Cai, Maosong Cao, Haojiong Chen, Kai Chen, Keyu Chen, Xin Chen, Xun Chen, Zehui Chen, Zhi Chen, Pei Chu, et al. Internlm2 technical report. *arXiv preprint arXiv:2403.17297*, 2024.
- [6] Lin Chen, Jisong Li, Xiaoyi Dong, Pan Zhang, Conghui He, Jiaqi Wang, Feng Zhao, and Dahua Lin. Sharegpt4v: Improving large multi-modal models with better captions. *arXiv preprint arXiv:2311.12793*, 2023.
- [7] Lin Chen, Jinsong Li, Xiaoyi Dong, Pan Zhang, Yuhang Zang, Zehui Chen, Haodong Duan, Jiaqi Wang, Yu Qiao, Dahua Lin, et al. Are we on the right way for evaluating large vision-language models? *arXiv preprint arXiv:2403.20330*, 2024.
- [8] Yangyi Chen, Xingyao Wang, Hao Peng, and Heng Ji. A single transformer for scalable vision-language modeling. *TMLR*, 2024.
- [9] Yi-Chia Chen, Wei-Hua Li, Cheng Sun, Yu-Chiang Frank Wang, and Chu-Song Chen. Sam4mllm: Enhance multimodal large language model for referring expression segmentation. *ECCV*, 2024.
- [10] Zhe Chen, Weiyun Wang, Yue Cao, Yangzhou Liu, Zhangwei Gao, Erfei Cui, Jinguo Zhu, Shenglong Ye, Hao Tian, Zhaoyang Liu, et al. Expanding performance boundaries of open-source multimodal models with model, data, and test-time scaling. *arXiv preprint arXiv:2412.05271*, 2024.
- [11] Zhe Chen, Jiannan Wu, Wenhai Wang, Weijie Su, Guo Chen, Sen Xing, Muyan Zhong, Qinglong Zhang, Xizhou Zhu, Lewei Lu, et al. Internvl: Scaling up vision foundation models and aligning for generic visual-linguistic tasks. In *CVPR*, 2024.
- [12] Bowen Cheng, Ishan Misra, Alexander G. Schwing, Alexander Kirillov, and Rohit Girdhar. Masked-attention mask transformer for universal image segmentation. In *CVPR*, 2022.
- [13] Jacob Devlin, Ming-Wei Chang, Kenton Lee, and Kristina Toutanova. Bert: Pre-training of deep bidirectional transformers for language understanding. In *ACL*, 2019.
- [14] Haiwen Diao, Yufeng Cui, Xiaotong Li, Yueze Wang, Huchuan Lu, and Xinlong Wang. Unveiling encoder-free vision-language models. *arXiv preprint arXiv:2406.11832*, 2024.
- [15] Haiwen Diao, Yufeng Cui, Xiaotong Li, Yueze Wang, Huchuan Lu, and Xinlong Wang. Unveiling encoder-free vision-language models. *NeurIPS*, 2025.
- [16] Haiwen Diao, Xiaotong Li, Yufeng Cui, Yueze Wang, Haoge Deng, Ting Pan, Wenxuan Wang, Huchuan Lu, and Xinlong Wang. Evev2: Improved baselines for encoder-free vision-language models. *arXiv preprint arXiv:2502.06788*, 2025.
- [17] Henghui Ding, Chang Liu, Suchen Wang, and Xudong Jiang. Vision-language transformer and query generation for referring segmentation. In *ICCV*, 2021.
- [18] Haodong Duan, Junming Yang, Yuxuan Qiao, Xinyu Fang, Lin Chen, Yuan Liu, Xiaoyi Dong, Yuhang Zang, Pan Zhang, Jiaqi Wang, et al. Vlmevalkit: An open-source toolkit for evaluating large multi-modality models. In *ACMMM*, 2024.
- [19] Guang Feng, Zhiwei Hu, Lihe Zhang, and Huchuan Lu. Encoder fusion network with co-attention embedding for referring image segmentation. In *CVPR*, 2021.
- [20] Chaoyou Fu, Peixian Chen, Yunhang Shen, Yulei Qin, Mengdan Zhang, Xu Lin, Jinrui Yang, Xiawu Zheng, Ke Li, Xing Sun, Yunsheng Wu, and Rongrong Ji. Mme: A comprehensive evaluation benchmark for multimodal large language models. *arXiv preprint arXiv:2306.13394*, 2023.
- [21] Xiuye Gu, Tsung-Yi Lin, Weicheng Kuo, and Yin Cui. Open-vocabulary object detection via vision and language knowledge distillation. In *ICLR*, 2022.
- [22] Louis Martin Hugo Touvron, Kevin Stone, Peter Albert, Amjad Almahairi, Yasmine Babaei, Nikolay Bashlykov, Soumya Batra, Prajjwal Bhargava, Shruti Bhosale, and et al. Llama 2: Open foundation and fine-tuned chat models. *arXiv:2307.09288*, 2023.
- [23] Tianrui Hui, Si Liu, Shaofei Huang, Guanbin Li, Sansi Yu, Faxi Zhang, and Jizhong Han. Linguistic structure guided context modeling for referring image segmentation. In *ECCV*, 2020.
- [24] Chao Jia, Yinfei Yang, Ye Xia, Yi-Ting Chen, Zarana Parekh, Hieu Pham, Quoc Le, Yun-Hsuan Sung, Zhen Li, and Tom Duerig. Scaling up visual and vision-language representation learning with noisy text supervision. In *ICML*, 2021.
- [25] Sahar Kazemzadeh, Vicente Ordonez, Mark Matten, and Tamara Berg. Referitgame: Referring to objects in photographs of natural scenes. In *EMNLP*, 2014.
- [26] Alexander Kirillov, Eric Mintun, Nikhila Ravi, Hanzi Mao, Chloe Rolland, Laura Gustafson, Tete Xiao, Spencer Whitehead, Alexander C Berg, Wan-Yen Lo, et al. Segment anything. *ICCV*, 2023.
- [27] Xin Lai, Zhuotao Tian, Yukang Chen, Yanwei Li, Yuhui Yuan, Shu Liu, and Jiaya Jia. Lisa: Reasoning segmentation via large language model. In *CVPR*, 2024.
- [28] Weixian Lei, Jiacong Wang, Haochen Wang, Xiangtai Li, Jun Hao Liew, Jiashi Feng, and Zilong Huang. The scalability of simplicity: Empirical analysis of vision-language learning with a single transformer. *arXiv*, 2025.
- [29] Bohao Li, Yuying Ge, Yixiao Ge, Guangzhi Wang, Rui Wang, Ruimao Zhang, and Ying Shan. Seed-bench: Benchmarking multimodal large language models. In *CVPR*, 2024.

- [30] Bo Li, Yuanhan Zhang, Dong Guo, Renrui Zhang, Feng Li, Hao Zhang, Kaichen Zhang, Yanwei Li, Ziwei Liu, and Chunyuan Li. Llava-onevision: Easy visual task transfer. *arXiv preprint arXiv:2408.03326*, 2024.
- [31] Junnan Li, Dongxu Li, Caiming Xiong, and Steven Hoi. Blip: Bootstrapping language-image pre-training for unified vision-language understanding and generation. In *ICML*, 2022.
- [32] Junnan Li, Dongxu Li, Silvio Savarese, and Steven Hoi. Blip-2: Bootstrapping language-image pre-training with frozen image encoders and large language models. In *ICML*, 2023.
- [33] Xiangtai Li, Haobo Yuan, Wei Li, Henghui Ding, Size Wu, Wenwei Zhang, Yining Li, Kai Chen, and Chen Change Loy. Omg-seg: Is one model good enough for all segmentation? In *CVPR*, 2024.
- [34] Xiaotong Li, Fan Zhang, Haiwen Diao, Yueze Wang, Xinlong Wang, and Ling-Yu Duan. Densfusion-1m: Merging vision experts for comprehensive multimodal perception. *arXiv preprint arXiv:2407.08303*, 2024.
- [35] Yanghao Li, Hanzi Mao, Ross Girshick, and Kaiming He. Exploring plain vision transformer backbones for object detection. *ECCV*, 2022.
- [36] Chen Liang, Wenguan Wang, Tianfei Zhou, Jiaxu Miao, Yawei Luo, and Yi Yang. Local-global context aware transformer for language-guided video segmentation. *arXiv preprint arXiv:2203.09773*, 2022.
- [37] Tsung-Yi Lin, Michael Maire, Serge Belongie, James Hays, Pietro Perona, Deva Ramanan, Piotr Dollár, and C Lawrence Zitnick. Microsoft coco: Common objects in context. In *ECCV*, 2014.
- [38] Weifeng Lin, Xinyu Wei, Ruichuan An, Peng Gao, Bocheng Zou, Yulin Luo, Siyuan Huang, Shanghang Zhang, and Hongsheng Li. Draw-and-understand: Leveraging visual prompts to enable mllms to comprehend what you want. *arXiv preprint arXiv:2403.20271*, 2024.
- [39] Chang Liu, Henghui Ding, and Xudong Jiang. GRES: Generalized referring expression segmentation. In *CVPR*, 2023.
- [40] Haotian Liu, Chunyuan Li, Qingyang Wu, and Yong Jae Lee. Visual instruction tuning. In *NeurIPS*, 2023.
- [41] Haotian Liu, Chunyuan Li, Yuheng Li, Bo Li, Yuanhan Zhang, Sheng Shen, and Yong Jae Lee. Llava-next: Improved reasoning, ocr, and world knowledge, 2024.
- [42] Jiang Liu, Hui Ding, Zhaowei Cai, Yuting Zhang, Ravi Kumar Satzoda, Vijay Mahadevan, and R Manmatha. Polyformer: Referring image segmentation as sequential polygon generation. *CVPR*, 2023.
- [43] Yuan Liu, Haodong Duan, Yuanhan Zhang, Bo Li, Songyang Zhang, Wangbo Zhao, Yike Yuan, Jiaqi Wang, Conghui He, Ziwei Liu, et al. Mmbench: Is your multi-modal model an all-around player? In *ECCV*, 2024.
- [44] Ilya Loshchilov and Frank Hutter. Decoupled weight decay regularization. *arXiv preprint*, 2017.
- [45] Timo Lüddecke and Alexander Ecker. Image segmentation using text and image prompts. In *CVPR*, 2022.
- [46] Gen Luo, Xue Yang, Wenhan Dou, Zhaokai Wang, Jifeng Dai, Yu Qiao, and Xizhou Zhu. Mono-intervl: Pushing the boundaries of monolithic multimodal large language models with endogenous visual pre-training. *CVPR*, 2025.
- [47] Chuofan Ma, Yi Jiang, Jiannan Wu, Zehuan Yuan, and Xiaojuan Qi. Groma: Localized visual tokenization for grounding multimodal large language models. In *ECCV*, 2024.
- [48] Shehan Munasinghe, Hanan Gani, Wenqi Zhu, Jiale Cao, Eric Xing, Fahad Shahbaz Khan, and Salman Khan. Videoglamm: A large multimodal model for pixel-level visual grounding in videos. *arXiv preprint arXiv:2411.04923*, 2024.
- [49] Lu Qi, Yi-Wen Chen, Lehan Yang, Tiancheng Shen, Xiangtai Li, Weidong Guo, Yu Xu, and Ming-Hsuan Yang. Generalizable entity grounding via assistance of large language model. *arXiv preprint arXiv:2402.02555*, 2024.
- [50] Alec Radford, Jong Wook Kim, Chris Hallacy, Aditya Ramesh, Gabriel Goh, Sandhini Agarwal, Girish Sastry, Amanda Askell, Pamela Mishkin, Jack Clark, et al. Learning transferable visual models from natural language supervision. In *ICML*, 2021.
- [51] Hanoona Rasheed, Muhammad Maaz, Sahal Shaji, Abdelrahman Shaker, Salman Khan, Hisham Cholakkal, Rao M. Anwer, Eric Xing, Ming-Hsuan Yang, and Fahad S. Khan. Glamm: Pixel grounding large multimodal model. In *CVPR*, 2024.
- [52] Jeff Rasley, Samyam Rajbhandari, Olatunji Ruwase, and Yuxiong He. Deepspeed: System optimizations enable training deep learning models with over 100 billion parameters. In *SIGKDD*, 2020.
- [53] Nikhila Ravi, Valentin Gabeur, Yuan-Ting Hu, Ronghang Hu, Chaitanya Ryali, Tengyu Ma, Haitham Khedr, Roman Rädle, Chloe Rolland, Laura Gustafson, et al. Sam 2: Segment anything in images and videos. *arXiv preprint arXiv:2408.00714*, 2024.
- [54] Zhongwei Ren, Zhicheng Huang, Yunchao Wei, Yao Zhao, Dongmei Fu, Jiashi Feng, and Xiaojie Jin. Pixellm: Pixel reasoning with large multimodal model. In *CVPR*, 2024.
- [55] Shengbang Tong, Ellis Brown, Penghao Wu, Sanghyun Woo, Manoj Middepogu, Sai Charitha Akula, Jihan Yang, Shusheng Yang, Adithya Iyer, Xichen Pan, Austin Wang, Rob Fergus, Yann LeCun, and Saining Xie. Cambrian-1: A fully open, vision-centric exploration of multimodal llms. In *NeurIPS*, 2024.
- [56] Hugo Touvron, Thibaut Lavril, Gautier Izacard, Xavier Martinet, Marie-Anne Lachaux, Timothée Lacroix, Baptiste Rozière, Naman Goyal, Eric Hambro, Faisal Azhar, Aurelien Rodriguez, Armand Joulin, Edouard Grave, and Guillaume Lample. Llama: Open and efficient foundation language models. *arXiv:2302.13971*, 2023.
- [57] Ramakrishna Vedantam, C Lawrence Zitnick, and Devi Parikh. Cider: Consensus-based image description evaluation. *CVPR*, 2015.
- [58] Jiaqi Wang, Pan Zhang, Tao Chu, Yuhang Cao, Yujie Zhou, Tong Wu, Bin Wang, Conghui He, and Dahua Lin. V3det: Vast vocabulary visual detection dataset. In *ICCV*, 2023.
- [59] Zhaoqing Wang, Yu Lu, Qiang Li, Xunqiang Tao, Yandong Guo, Mingming Gong, and Tongliang Liu. Cris: Clip-driven referring image segmentation. In *CVPR*, 2022.

- [60] Cong Wei, Haoxian Tan, Yujie Zhong, Yujiu Yang, and Lin Ma. LaSagnA: Language-based segmentation assistant for complex queries. *arXiv preprint arXiv:2404.08506*, 2024.
- [61] Jianzong Wu, Xiangtai Li, Shilin Xu, Haobo Yuan, Henghui Ding, Yibo Yang, Xia Li, Jiangning Zhang, Yunhai Tong, Xudong Jiang, Bernard Ghanem, and Dacheng Tao. Towards open vocabulary learning: A survey. *arXiv pre-print*, 2023.
- [62] Size Wu, Sheng Jin, Wenwei Zhang, Lumin Xu, Wentao Liu, Wei Li, and Chen Change Loy. F-lmm: Grounding frozen large multimodal models. *CVPR*, 2025.
- [63] Zhuofan Xia, Dongchen Han, Yizeng Han, Xuran Pan, Shiji Song, and Gao Huang. Gsva: Generalized segmentation via multimodal large language models. In *CVPR*, 2024.
- [64] Hu Xu, Saining Xie, Xiaoqing Ellen Tan, Po-Yao Huang, Russell Howes, Vasu Sharma, Shang-Wen Li, Gargi Ghosh, Luke Zettlemoyer, and Christoph Feichtenhofer. Demystifying clip data. *arXiv preprint arXiv:2309.16671*, 2023.
- [65] An Yang, Baosong Yang, Binyuan Hui, Bo Zheng, Bowen Yu, Chang Zhou, Chengpeng Li, Chengyuan Li, Dayiheng Liu, Fei Huang, Guanting Dong, Haoran Wei, Huan Lin, Jialong Tang, Jialin Wang, Jian Yang, Jianhong Tu, Jianwei Zhang, Jianxin Ma, Jin Xu, Jingren Zhou, Jinze Bai, Jincheng He, Junyang Lin, Kai Dang, Keming Lu, Keqin Chen, Kexin Yang, Mei Li, Mingfeng Xue, Na Ni, Pei Zhang, Peng Wang, Ru Peng, Rui Men, Ruize Gao, Runji Lin, Shijie Wang, Shuai Bai, Sinan Tan, Tianhang Zhu, Tianhao Li, Tianyu Liu, Wenbin Ge, Xiaodong Deng, Xiaohuan Zhou, Xingzhang Ren, Xinyu Zhang, Xipin Wei, Xuancheng Ren, Yang Fan, Yang Yao, Yichang Zhang, Yu Wan, Yunfei Chu, Yuqiong Liu, Zeyu Cui, Zhenru Zhang, and Zhihao Fan. Qwen2 technical report. *arXiv preprint arXiv:2407.10671*, 2024.
- [66] An Yang, Baosong Yang, Beichen Zhang, Binyuan Hui, Bo Zheng, Bowen Yu, Chengyuan Li, Dayiheng Liu, Fei Huang, Haoran Wei, et al. Qwen2.5 technical report. *arXiv preprint arXiv:2412.15115*, 2024.
- [67] Zhao Yang, Jiaqi Wang, Yansong Tang, Kai Chen, Hengshuang Zhao, and Philip HS Torr. Lavt: Language-aware vision transformer for referring image segmentation. In *CVPR*, 2022.
- [68] Zhao Yang, Jiaqi Wang, Yansong Tang, Kai Chen, Hengshuang Zhao, and Philip HS Torr. Lavt: Language-aware vision transformer for referring image segmentation. In *CVPR*, 2022.
- [69] Zuyao You, Junke Wang, Lingyu Kong, Bo He, and Zuxuan Wu. Pix2cap-coco: Advancing visual comprehension via pixel-level captioning. *arXiv preprint arXiv:2501.13893*, 2025.
- [70] Licheng Yu, Patrick Poirson, Shan Yang, Alexander C Berg, and Tamara L Berg. Modeling context in referring expressions. In *ECCV*, 2016.
- [71] Haobo Yuan, Xiangtai Li, Chong Zhou, Yining Li, Kai Chen, and Chen Change Loy. Open-vocabulary sam: Segment and recognize twenty-thousand classes interactively. *arXiv preprint*, 2024.
- [72] Haobo Yuan, Xiangtai Li, Tao Zhang, Zilong Huang, Shilin Xu, Shunping Ji, Yunhai Tong, Lu Qi, Jiashi Feng, and Ming-Hsuan Yang. Sa2va: Marrying sam2 with llava for dense grounded understanding of images and videos. *arXiv preprint arXiv:2501.04001*, 2025.
- [73] Haobo Yuan, Tao Zhang, Xiangtai Li, Lu Qi, Zilong Huang, Shilin Xu, Jiashi Feng, and Ming-Hsuan Yang. 4th pvuw mevis 3rd place report: Sa2va. *arXiv preprint arXiv:2504.00476*, 2025.
- [74] Yuqian Yuan, Wentong Li, Jian Liu, Dongqi Tang, Xinjie Luo, Chi Qin, Lei Zhang, and Jianke Zhu. Osprey: Pixel understanding with visual instruction tuning. In *CVPR*, 2024.
- [75] Alireza Zareian, Kevin Dela Rosa, Derek Hao Hu, and Shih-Fu Chang. Open-vocabulary object detection using captions. In *CVPR*, 2021.
- [76] Xiaohua Zhai, Basil Mustafa, Alexander Kolesnikov, and Lucas Beyer. Sigmoid loss for language image pre-training. In *ICCV*, 2023.
- [77] Pan Zhang, Xiaoyi Dong, Bin Wang, Yuhang Cao, Chao Xu, Linke Ouyang, Zhiyuan Zhao, Shuangrui Ding, Songyang Zhang, Haodong Duan, Wenwei Zhang, Hang Yan, Xinyue Zhang, Wei Li, Jingwen Li, Kai Chen, Conghui He, Xingcheng Zhang, Yu Qiao, Dahua Lin, and Jiaqi Wang. Internlm-xcomposer: A vision-language large model for advanced text-image comprehension and composition. *arXiv preprint arXiv:2309.15112*, 2023.
- [78] Tao Zhang, Xingye Tian, Yu Wu, Shunping Ji, Xuebo Wang, Yuan Zhang, and Pengfei Wan. DVIS: Decoupled video instance segmentation framework. In *ICCV*, 2023.
- [79] Tao Zhang, Xingye Tian, Yikang Zhou, Shunping Ji, Xuebo Wang, Xin Tao, Yuan Zhang, Pengfei Wan, Zhongyuan Wang, and Yu Wu. Dvis++: Improved decoupled framework for universal video segmentation. *arXiv preprint arXiv:2312.13305*, 2023.
- [80] Tao Zhang, Xiangtai Li, Hao Fei, Haobo Yuan, Shengqiong Wu, Shunping Ji, Change Loy Chen, and Shuicheng Yan. Omg-llava: Bridging image-level, object-level, pixel-level reasoning and understanding. In *NeurIPS*, 2024.
- [81] Yichi Zhang, Ziqiao Ma, Xiaofeng Gao, Suhaila Shakiah, Qiaozhi Gao, and Joyce Chai. Groundhog: Grounding large language models to holistic segmentation. In *CVPR*, 2024.
- [82] Yikang Zhou, Tao Zhang, Shilin Xu, Shihao Chen, Qianyu Zhou, Yunhai Tong, Shunping Ji, Jiangning Zhang, Xiangtai Li, and Lu Qi. Are they the same? exploring visual correspondence shortcomings of multimodal llms. *arXiv preprint arXiv:2501.04670*, 2025.

Pixel-SAIL: Single Transformer For Pixel-Grounded Understanding

Supplementary Material

We first present more details on training and testing of our Pixel-SAIL in Sec. 6. Then, we present the detailed benchmark building process, in Sec. 7 and more challenging examples in PerBench in Sec. 8. Next, we present more comparison with current state-of-the-art pixel-grounded MLLMs, in Sec. 9.

6. More Detailed Training and Testing

Training. We will present more details about the training, including dataset sampling specifications and distillation methodology. For the RefCOCO series [25, 70] datasets, we randomly sample 5 referring expressions per image and organize them into a multi-round dialogue format as a single training data point, processing all images for four epochs. For COCO [37] data, we sample 5 categories per image and randomly select either instance mode or semantic mode to structure the responses. In instance mode, objects are arranged by their center points from left to right. We process the COCO dataset for one epoch. For Pixel2Cap [69], our generated detailed object caption data, and Osprey [74] object description data, we randomly sample 1-5 visual prompts per image and randomly incorporate questions about non-existent visual prompts, with responses indicating that these visual prompts do not exist. These object caption datasets are processed for five epochs. For other segmentation-related or visual prompt-related data, we conduct one epoch. For LLaVA-665k, we randomly sample at a 1:1 ratio alongside other data for joint training to ensure that the base MLLM’s instruction-following capability remains intact.

When the length of input tokens (including the length of vision tokens) exceeds 8192, we truncate the excess portion. For the 0.5B model, we use DeepSpeed Zero-1 [52] for training, and for the 3B and 7B models, we use DeepSpeed Zero-2 [52] for training.

We distill the mask features generated by the Mask2Former [12] pixel decoder and the lowest resolution features generated by the SAM2 [53] image encoder onto the upsampled mask features from Pixel-SAIL and the image features directly reshaped from vision tokens, respectively. We use bilinear interpolation to align spatial dimensions and implement a learnable linear layer to align the channel size. The distillation process employs MSE loss with a weight of 0.5.

Testing. We have elaborated on the testing details of Pixel-SAIL on pixel-grounded benchmarks in the main text. For general image question answering benchmarks, we follow the prompt settings of the base MLLMs and use

VLMEvalKit [18] for evaluation, without using additional LLM assistance to identify answers.

7. More Detailed Process on Benchmarking Building

The construction of PerBench combines an automated model-generated pipeline with manual screening, correction, and annotation. The process is divided into three stages.

The **first stage** involves annotating detailed object captions. We crop objects and draw visual prompts on the original images to prompt InternVL-2.5 78B [10] and Qwen-VL 2.5 72B [2] to generate detailed captions for the objects. These captions are then cross-validated using Qwen2.5 72B [66]. If all captions are consistent, they are integrated using an LLM; otherwise, the data are discarded. After the model automatically generates the detailed object captions, we manually select and correct 500 of them to form the final 500 detailed object caption data points in the benchmark.

The **second stage** focuses on annotating visual-prompt question-answering data in an MCQ (Multiple Choice Question) format. In this phase, we manually generate a multiple-choice question for each object caption obtained from the first stage. After completing the annotations, two quality control specialists perform cross-verification to identify and rectify any potential errors.

The **final stage** contains the annotation of visual-text referring segmentation data. At this stage, we manually select and annotate object segmentation masks, referring visual prompts, and text from SAM images. During the annotation process, we consider various factors such as positional relationships, event relationships, appearance, size, and more, including cases with both single and multiple visual prompts. Once the annotation is complete, two individuals review it, and correct the errors.

8. More Challenging Cases in PerBench

We present more detailed object caption samples from our PerBench in Fig. 6. The objects are derived from diverse senses and categories, encompassing humans, man-made objects, and natural landscapes. The object captions include basic categories, attributes, purposes, and relationships with surrounding objects. This high-quality benchmark will effectively advance the development of the visual prompt understanding community.

More referring segmentation samples are illustrated in Fig. 7. Our manually annotated samples cover a variety of scenes, such as indoor and outdoor settings, and include



The object is a person standing behind a wooden podium covered with a blue cloth, addressing an audience outdoors. The podium has an emblem, and the person is dressed in a dark blue jacket with a logo, a scarf, and a white shirt. The audience includes people seated on a stool and a folding chair, with trees, parked cars, and a building with large windows visible in the background.



The object is a bronze statue of a young boy with exaggerated features. The statue is dressed in a formal outfit including a suit jacket, vest, and shorts, and it wears flip-flops. The boy holds a small object resembling a ball in his right hand. The statue's whimsical and playful appearance, characterized by exaggerated proportions and a sense of movement, is set on a rock-like structure in an urban street scene with a pedestrian crossing visible in the background.



The object is a person dressed in black and blue attire, standing on skis in a snowy outdoor setting, preparing for or participating in a skiing event. This person is wearing a black beanie, a black puffy jacket, black gloves, black pants, and a blue bib with the number "1" in red. They also have ski poles and ski boots. In the background, there are other people skiing or standing around, along with parked cars and trees, indicating a recreational or competitive skiing area.



The object is a Smart Fortwo, a compact city car known for its small size and maneuverability. This car features predominantly white with green accents, including green wheels and trim. Designed for urban environments with limited parking space, it is parked on a sidewalk next to a charging station, indicating its electric vehicle status. The charging cable is connected, suggesting it is currently being charged. The surrounding area includes a paved road with multiple lanes and a grassy area separated by a curb.



The object is a stack of white bangles adorned with small, colorful stones. These bangles, part of traditional jewelry, are worn on the arm of a person dressed in vibrant traditional attire, including a yellow scarf with colorful patterns and a floral-patterned garment, complementing the overall colorful and cultural appearance.



The object is a waterfall cascading down a steep, rocky cliff. The waterfall serves as the central focus, with water flowing smoothly from top to bottom. The area around the waterfall features rugged, uneven rock surfaces and patches of green vegetation. The cliff is part of a larger mountainous or hilly terrain, with dense foliage at the top. The waterfall's flow and movement create a striking contrast against the dark, textured rocks, highlighting the natural beauty of the scene.



The object is a black shoulder bag with a flap closure. It is made of a synthetic or leather-like material, has a smooth texture and sheen, and is carried over the shoulder of a person walking in a grassy area near a wooden fence and a small white stool, dressed in a black top and pink shorts.

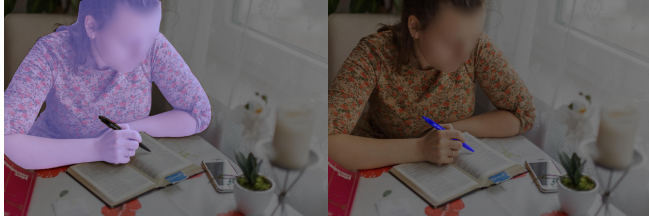


The object is a navigational buoy used in maritime environments. It is a cylindrical structure with a pointed top, primarily white in color, featuring a pink top and a distinctive band. Mounted on a black base, it is situated in a body of water such as a harbor or marina, surrounded by other boats and buoys. Its function is to guide vessels through waterways, aiding navigation with its unique color pattern. This buoy is part of a larger maritime setting, often near populated areas or popular boating destinations.

Figure 6. More visualization examples of detailed object captions from our PerBench.

objects of multiple granularities. The referring text encompasses positional relationships, event relationships, and more. This new task is more challenging than current pure text referring segmentation tasks.

Q: Please segment which object <vp_0> is using. A: [SEG]



Q: Please segment the <vp_0> that is sitting. A: [SEG]



Q: Please segment where <vp_0> will arrive. A: [SEG]



Q: Please segment the object that blocks the sunlight for <vp_0>. A: [SEG]



Q: Please segment the letter closest to <vp_0>. A: [SEG]



Q: Please segment the object that <vp_0> is enjoying. A: [SEG]



Q: Please segment the person who is holding <vp_0>. A: [SEG]



Q: Please segment the tree between <vp_0> and <vp_1>. A: [SEG]



Figure 7. More visualization examples of vision-text referring segmentation from our PerBench.

9. More Comparison With SOTA Pixel-Grounded MLLM

We conduct a qualitative comparative analysis with the SOTA pixel-grounded MLLM, Sa2VA [72], and present the visualization results in Fig. 8. We observe that both Pixel-SAIL and Sa2VA achieve excellent results in most cases. However, Sa2VA performs significantly weaker than Pixel-SAIL in certain scenarios, despite utilizing the much more powerful InternVL2.5 [10] compared to our base encoder-free MLLM [8]. In the left examples, Sa2VA performs notably worse than Pixel-SAIL in multi-object segmentation

tasks. Additionally, in the right example, Sa2VA demonstrates significantly weaker attention to non-core areas of the image, such as edges, compared to Pixel-SAIL, leading to frequent failures in segmenting objects near image boundaries.



Figure 8. Visualization Comparison of Sa2Va and Pixel-SAIL.